Additive-Subtractive Process Chain for Highly Functional Polymer Components

Michael Baranowski [1], Nikolas Matkovic [1,*], Sebastian Kleim [1], Marco Friedmann [1], Jürgen Fleischer [1], Marlies Springmann [2], Peter Middendorf [2], Adrian Schäfer [3], Marcel Waldhof [3], and Nejila Parspour [3]

[1] WBK Institute of Production Science, Karlsruhe Institute of Technology (KIT), Karlsruhe, Germany;
Email: michael.baranowski@kit.edu (M.B.), marco.friedmann@kit.edu (M.F.), juergen.fleischer@kit.edu (J.F.), sebastian.kleim@student.kit.edu (S.K.)
[2] IFB-Institute of Aircraft Design, University of Stuttgart, Stuttgart, Germany;
Email: springmann@ifb.uni-stuttgart.de (M.S.), middendorf@ifb.uni-stuttgart.de (P.M.)
[3] IEW-Institute of Electrical Energy, University of Stuttgart, Stuttgart, Germany;
Email: adrian.schaefer@iew.uni-stuttgart.de (A.S.), marcel.waldhof@iew.uni-stuttgart.de (M.W.), nejila.parspour@iew.uni-stuttgart.de (N.P.)
*Correspondence: nikolas.matkovic@kit.edu (N.M.)

***Abstract*—Additive manufacturing processes offer the possibility of producing components without using tools. Especially in mobility, new technologies are needed to make geometrically complex, functionally integrated and highly precise components. The Fused Filament Fabrication (FFF) process is an additive manufacturing technique that offers easy handling and a large range of materials. However, the FFF process has a considerable shortcoming in dimensional accuracy. A process hybridization consisting of additive and subtractive steps was developed to eliminate this shortcoming. Applying subtractive work steps enables the precise integration of inserts and, thus, the production of highly functional polymer components. For this purpose, suitable demonstrators are derived from an example of a stator of a double-sided axial flux machine and the manufacturing process with the different working steps (additive & subtractive) is demonstrated. The focus is on increasing the dimensional accuracy and more precise integration of the inserts with the help of subtractive steps. Furthermore, non-planar overprinting during the additive manufacturing steps was investigated. The advantages of the combination of subtractive processing and non-planar printing were concluded.**

***Keywords*—automated additive-subtractive manufacturing process, manufacturing accuracy of FFF-components, insert integration**

I. Introduction

The increasing integration of different functions in a single component generally reduces the number of parts needed to fulfill the requirements of the end product. Furthermore, manufacturing effort and costs decrease, as fewer steps are required in production and assembly.

In the field of electric drives, for example, this approach offers the potential to increase the performance of the resulting system, because various requirements from different physical domains are placed on the single components used. For electric motors, mechanical, thermal, electrical and magnetic requirements occur. In addition, intelligent functions are increasingly being realized with the aid of sensors, which can be used to monitor the condition of the component and increase its efficiency.

To meet these requirements in the best possible way, there is a need for a manufacturing process in which components are produced cost-efficiently with a high degree of dimensional freedom and enabling the combination of different materials, as well as the integration of additional subcomponents. Therefore, a new manufacturing process combining the additive fused Filament Fabrication Process (FFF) with the subtractive milling process and an automated assembly device is presented here.

By applying molten polymer wire (filament) layer by layer, the FFF process enables the cost-efficient manufacturing of components with a high degree of dimensional freedom and also offers the possibility of incorporating additional intermediate steps into the manufacturing process. In this way, the disadvantages of the FFF process, which include a lower accuracy and a lower strength, can be mitigated during production. Subtractive intermediate steps specifically increase the accuracy of the resulting component. In addition, this enables the precise integration of inserts made of other materials or subcomponents, thus increasing the functional scope of the resulting component.

II. Basics and State of Research & Technology

A. Double-Sided Axial Flux Machine

The development of a flexible manufacturing process requires a demonstration object for the application and validation of the individual process steps as well as the

Manuscript received January 6, 2023; revised April 19, 2023; accepted June 6, 2023.

order of the steps. In this case, the stator of a double-sided axial flux machine is used (see Fig. 1), as this type of machine is getting increasing attention due to its advantages (e.g., high torque density) compared to the common radial flux machine [1–3]. Furthermore, the axial alignment of the stator teeth is advantageous for testing the manufacturing process [4]. Because the stator yoke is missing for this particular machine design, there must be an additional structure which establishes the mechanical connection between the separated stator segments [5]. Either metal structures are used, which can lead to additional eddy current losses [6], or epoxy potting techniques are used, which complicate the connection to the cooling system, requiring additional measures to reduce thermal resistance [5, 7]. Therefore, in this work a different approach is proposed. The housing of the stator is printed with the FFF process and additional components, e.g., a heat sink, are integrated into it. So, the wide range of requirements from different physical domains shall be met. Due to the high level of integration, there is the potential to handle the challenges with the mechanical and thermal connection at once.

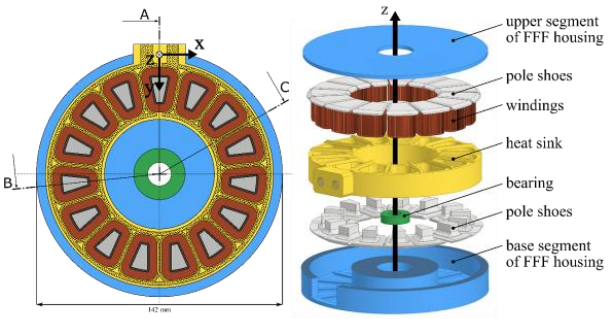

Figure 1. Stator of a double-sided axial flux machine [4].

Electrical machines are electromechanical energy converters, which is why electrical conductors, such as copper, with high electrical conductivity, are required to create a magnetic field. Moreover, soft magnetic materials, such as iron, with high magnetic conductivity are required to guide the magnetic field within the machine [8]. As the equations of the electromagnetic torque by [1, 3] suggest, the torque is linearly dependent on the area of the air gap. In order to increase the resulting torque, the magnetic field must be guided through an air gap with a large area. To achieve this large area for this type of machine the field must be guided not only in a two dimensional-plane but in the three-dimensional space [9]. Consequently, the arrangement, insertion and connection of the soft magnetic materials pose a challenge with this type of machine, which is to be solved by the hybrid manufacturing process. Furthermore, the inaccurate alignment and positioning of the soft magnetic materials leads to uneven field distributions and thus to torque fluctuations and additional loads [10]. This is why the accuracy of subtractive finishing is essential here.

Moreover, electric and magnetic losses occur during the operation of an electrical machine, which represent a heat source within the stator [11]. The resulting temperatures, combined with the permissible maximum temperatures of the materials, are decisive for the maximum operating power [12]. At comparatively low speeds the copper windings are the main source of heat and therefore need direct cooling to keep the temperatures low and protect the machine from thermal destruction [12]. For electrical machines the two most important effects in the dissipation of the heat flow are conduction and convection. Both effects are improved by increasing the transfer area. Conduction is improved further by decreasing the transfer length [13].

There are three main approaches regarding the cooling concept of the axial flux machine. Because a heat sink with a cooling liquid is more efficient than cooling with air [14] all three approaches are using a liquid as coolant. In the first approach a standard cooling jacket with cooling channels is placed on the outer circumference of the stator and the contact to the coils is established with additional heat conducting structures [5]. This still leaves a comparatively long heat transfer path, a small transfer area, and potentially leads to additional eddy currents. Therefore, in the second approach the liquid directly contacts the coils, maximizing the transfer area and minimizing the transfer length, thereby achieving the best cooling effect in comparison [15]. Because the stator mostly is filled with liquid the mechanical connection of the stator segments and the sealing of the liquid volume are challenging for the direct cooling approach [16]. Lastly, a combined approach exists, where the cooling channels in the heat sink are routed to the coils and the zones between the stator segments [16]. This approach leads to an elaborate manufacturing, high pressure losses and additional eddy currents [16]. Hence, for this demonstration concept the approaches two and three are combined. The heat sink is additively manufactured from an electric nonconductive material suppressing eddy currents. The heat sink is sealed, still allowing the mechanical connection, and imitating the guidance of the coolant from the direct liquid cooling, so a similar thermal performance is expected. For the demonstration of the manufacturing process the heat sink is manufactured with the stereolithography (SLA) process beforehand and inserted into the stator during production. The subtractive process step ensures a precise fit of the heat sink within the FFF housing, thereby facilitating the automated insertion process. The FFF housing is manufactured from polylactide (PLA) to ensure good adhesion to the SLA heat sink [17]. In the future the heat sink must be additively manufactured from a polymer with increased thermal conductivity [18] or from ceramics [19] to overcome the bottleneck of the high thermal resistance of the wall. The FFF housing should be made of thermoplastics with higher stiffness, e.g., short-fiber reinforced polyamide 6.

Finally, the mechanical properties of the stator are considered: On the one hand, the stator can be strengthened by introducing additional materials, and on the other hand, the rotor of the machine must be guided in the stator. Commercially available bearings can be used for this purpose, which are integrated directly during manufacturing. The alignment of a pair of bearings to each

other is important for the smooth running of the machine. The required accuracy is realizable with the aid of the milling process.

B. Hybrid Process Chains in Additive Manufacturing

In the current state of research and technology, some process chains exist for hybrid additive manufacturing of highly functional components. In this context, "hybrid" means the combination of additive manufacturing with a further manufacturing process from a different main manufacturing group of DIN 8580 [20]. The aim is to combine the manufacturing processes' advantages or eliminate the disadvantages of the other manufacturing process. For example, in [21–24], the additive manufacturing process is used to build the basic structure of the component. However, additively manufactured parts have a relatively low surface quality and a low dimensional accuracy [25]. To eliminate these disadvantages, the components' surface quality and dimensional accuracy are reworked in a targeted manner with the aid of a milling process in the same machine.

Society's increasing demand for individualisation requires more functional integration [26]. In this context, function integration extends a component's functional scope by integrating external elements (e.g., sensors, LEDs, conductors, nuts, metal inserts, and threads) into additively manufactured component structures [27–29]. In [18, 30–36], approaches are presented on how, for example, electrical components are integrated into the printed part with the help of pick and place kinematics and contacted with the use of conductive pastes or filaments.

Another trend is the additive manufacturing of multi-material designs according to the principle of "functional material at functional location" [17]. In the future, components must, for example, have high local strength and elasticity at other points. Furthermore, thermal or electrical conductivity or insulation is required in the same part [25, 26].

However, for the flexible and economical production of highly integrated components in variable quantities, no machine technology currently enables a combination of hybrid, additive-subtractive production of multi-material components and automated functional integration. As part of the Innovation Campus - Mobility of the Future, a new type of machine (4K FFF Machine - see next chapter) was developed to enable the seamless production of highly integrated functional components [37]. With the help of this machine, the degree of automation and flexibility for the production of future components is to be maximised, and at the same time, the production time and costs are to be reduced.

C. 4K FFF Machine

The machine consists of an FFF-printing module with four extrusion nozzles (multi-material printing–4K), four motion axes (x, y, z, C) and a handling robot for the integration of sub-components see Fig. 2. To increase the dimensional and shape accuracy of the printed components and to reduce the clearance between the sub-component and the FFF structure, a milling module was integrated into the system [38].

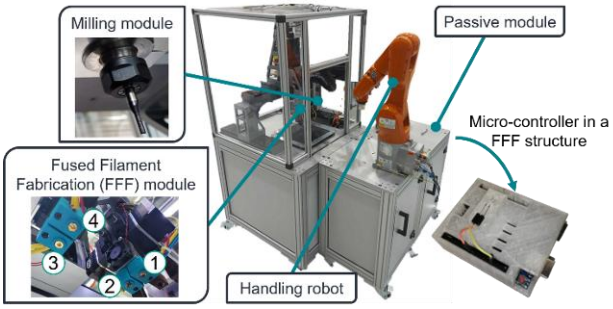

Figure 2. 4K FFF machine.

Table I below lists the machine's technical data shown in Fig. 2.

TABLE I. FEATURES OF THE 4K FFF MACHINE

Feature	Description
Mechanical structure	In-house development
Axes of motion	x, y, z, C
PLC & CNC	Beckhoff CX5140-0175
Inline quality assurance	Image processing (2D)
Nozzles	4 × E3D Hemera extruder and nozzles
Build volume	250 × 210 × 150 mm^3 (l × b × h)
Milling spindle	AMB 1050 FME-P DI 230V
Milling tool	End mill made of carbide and two cutting edges (Ø 2 mm)
Robot + Control	KUKA KR6 HA + KRC4
Communication between FFF printer and robot	Serial interface and from the basis of the information within the CNC code (position data)
Slicing of FFF part	Ultimaker Cura
Materials	PLA, ABS, PETG, PA, …
Planning of process steps and process sequence	HybridPlaner (HP)
Chip removal during machining	Compressed air

Fig. 3 shows the primary sequence for producing parts with the 4K FFF machine.

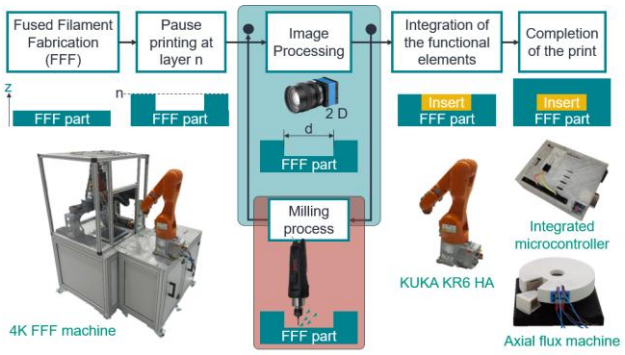

Figure 3. Process flow of the 4K FFF machine.

The basic structure is produced in the first step using the FFF process (see Fig. 3). The cavity, i.e., the negative shape of the part to be integrated, is already provided in the CAD model and is not filled with a support structure during the printing process. In a layer defined by the user, the printing process is paused at the machine's zero point, and thus the measurement of the cavity is started using a

camera. An external image processing program compares the target dimension with the actual dimension. The difference or the remaining oversize is transferred to the control of the FFF module and converted into a milling cycle (circular pocket, rectangular pocket, etc.). At the end of the milling cycle, the pocket is rechecked. If the pocket is too large, i.e., the dimension of the pocket is out of tolerance, the machine goes into standby mode. The user receives an e-mail notification of the current machine status. The industrial robot is activated if the cavity is within the specified tolerances. The robot picks up the insert to be placed using a gripper (suction gripper, parallel jaw gripper or similar) on the passive module provided.

For process planning of the individual process steps (printing, milling, handling, image processing), the MATLAB-based application HybridPlaner (HP) was developed [39]. The development of the process planning tool is motivated by the fact that there has been no universal software for hybrid additive manufacturing planning or software adapted to the machine concept of the 4K FFF machine. The input of the HP is a g-code, which can be taken from any slicer (e.g., open-sorce slicer like Cura, Prusa or in-house slicer with planar and non-planar layer planning). This g-code is then converted into DIN-compliant language in the HP. The HP provides the operator with a graphical user interface (HMI) that allows it to plan the manufacturing process with all necessary steps interactively. The result of the process planning and output of the HP is an extended file with the CNC code executable by the 4K FFF machine [4].

D. Research Deficit & Objective

The 4K FFF machine presented here forms a promising basis for the automated production of highly integrated functional components in multi-material construction. However, the developed machine has not yet been analyzed and optimized for manufacturing accuracy (combination of multi-material printing and milling), and the potential cannot yet be fully exploited. The current 4K FFF Machine has a low manufacturing accuracy (maximum deviation 0.1–0.3 mm) because the four extrusion nozzles and the milling spindle are not precisely aligned and measured in relation to each other. The results are components with increased shape and dimensional inaccuracies. Although the state of research and technology offers various possibilities to optimize the individual sub-processes (FFF process, milling process) independently of each other with the help of test components (benchmark parts) [25, 40–42], there is no method for examining and optimizing the working accuracy for such additive-subtractive FFF hybrid processes.

The first objective is therefore to carry out an indirect metrological investigation of the 4K FFF Process with the help of a developed test workpiece to increase the shape and dimensional accuracy of the manufactured components. With the help of this investigation, existing deviations between the installed milling module and a pair of nozzles (No. 1, 2) are to be determined and eliminated. Through the experimental production of the designed stator of a double-sided axial flux machine, the added value of the improved system accuracy is to be demonstrated in the second objective.

III. Experimental Setup

A. Indirect Measurement Analysis

The self-developed 4K FFF Machine has an industrial Programmable Logic Controller (PLC) from Beckhoff with CNC extension according to DIN 66025 [43] or ISO 6983 [44]. Due to the kinematics, i.e., three linear axes (x, y, and z) for moving the nozzles and a rotation axis (C) for rotating the building platform, this machine can be considered a machine tool according to the definition in [45]. In [45], indirect metrological examinations are used to determine the working accuracy of machine tools. In such investigations, a clear statement about the working accuracy can be made by producing test workpieces. Following [45], the test workpiece shown in Fig. 4 was developed.

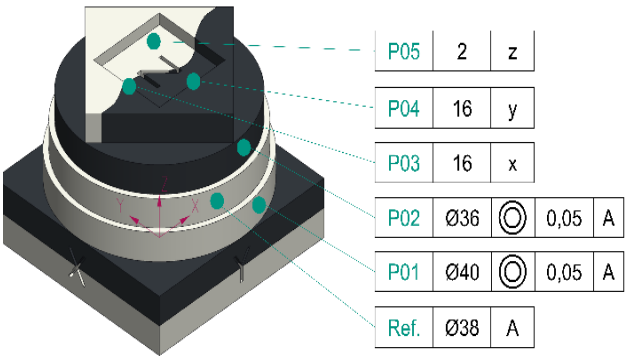

Figure 4. Test workpiece for the 4K FFF process.

The individual test features in Fig. 4 optimizing the working accuracy for nozzle 1 and nozzle 2 are listed and described in Table II. A coordinate measuring machine (Zeiss O-Inspect) was used to measure these test features.

TABLE II. Features of the Test Workpiece

Feature	Description (values in millimeters)
Ref.	Printed Circle Ø38.00 / Nozzle 1 / PLA white
P01	Concentricity Ø40 to P01 / milled / finishing allowance 0.3
P02	Concentricity Ø36 to P01 / Printed Circle / Nozzle 2 / PLA black conductive
P03	Pocket length 16.00 / milled / finishing allowance 0.3
P04	Pocket width 16.00 / milled / finishing allowance 0.3
P05	Pocket depth 2.00 / milled / finishing allowance 0.2

By selecting these test features, on the one hand, the distance of the nozzles can be corrected via the concentricity of the cylinders or collinearity of the cylinder axes and on the other hand, the distance of the reference nozzle (nozzle 1) to the milling tool can be determined. After measuring the deviation, an increase in the dimensional and form accuracy can be achieved by a cutter length and cutter radius compensation in the CNC control. By substituting nozzle two with nozzle three or nozzle four, the working accuracy for the other nozzles can be increased. The optimization of nozzle three and nozzle

four, and different component dimensions will not be discussed further in this paper.

The white material made of PLA (Formfortuna EasyFil) of the test workpiece is created by nozzle 1 (reference nozzle). The black material consisted of conductive PLA (Proto-Pasta, conductive) and was created by nozzle 2. The machine parameters, according to Table III, were used as machine settings.

TABLE III. PRINTER SETTINGS (4K FFF MACHINE)

Process parameters	Value with unit
Print temperature nozzle 1 / nozzle 2	210 ℃ / 210 ℃
Part bed temperature	75 ℃
Layer height	0.2 mm
Infill	20%
Print speed	40 mm/s
Retraction speed	45 mm/s
Retraction distance	3 mm
Milling tool	2 mm end mill
Milling speed	15,000 1/min
Milling feed rate	3,000 mm/min

First, the actual condition of the system was determined, and the deviation from the target values was derived. After correcting the measured deviations in the CNC control (tool radius correction, distances between nozzles and milling cutter, extension length of the milling cutter), a new test workpiece was produced.

B. *Additive-Subtractive Production of the Highly Functional Stator and Sub-demonstrator*

A flexible slicing strategy was developed in [4] to combine the additive and subtractive manufacturing steps. Here, an existing component is divided into individual segments and g-codes are generated for each segment. Depending on the geometry requirements of the individual segments, a planar or non-planar slicing principle is applied. A non-planar slicing strategy signifies that the layers are not flat, but follow the curvature of the inserts. This prevents the stair-stepping effect at the interface between the FFF component and the insert and results in better adhesion between the individual components. With the help of a Matlab script, the individual g-codes of the segments are stacked and additional so-called breakpoints are inserted. At these breakpoints, an optical measurement, subtractive processing or an insert integration can be performed. This g-code determines the printing order of the layers of the individual segments and contains a collision avoidance, especially when switching between non-planar and planar layers. An additional collision avoidance strategy is necessary because the general collision avoidance, as in the case of a completely planar layer structure, is no longer given. For the detailed process planning of the additional steps at the breakpoints (milling, handling, image processing), the g-code is extended via the HybridPlaner as mentioned before.

The described stator was examined with regard to areas with high dimensional accuracy requirements. The ribs for positioning the heat sink and pole shoes were identified as critical (see Fig. 5 red area). Therefore, a simpler sub-demonstrator was derived. Fig. 5 shows the demonstrator for replicating the area around the heat sink and pole shoes. The sub-demonstrator depicts the situation in the area of the ribs for positioning the heat sink and the pole shoes. Here, a non-planar layer design is implemented in the upper area of the chamfers to minimize the stair-stepping effect. For a gapless insertion of the heat sinks and the pole shoe two different strategies are investigated. First the lower chamfer is built up with a planar and a non-planar printing strategy. Subsequently, the influence of the printing strategies on the number of gaps in the interface is investigated. As an additional step, the interface of the lower chamfer is refinished with the help of a subtractive manufacturing step (Milling). By eliminating the stair-stepping effects, intimate contact between the FFF area and the heatsink is improved for effective cooling.

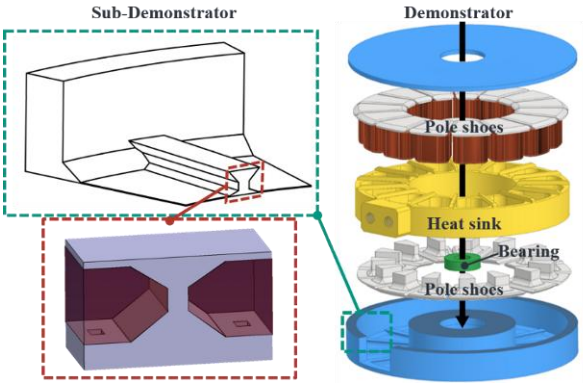

Figure 5. Demonstrator and derived sub-demonstrator.

The individual steps of the additive-subtractive manufacturing of the sub-demonstrator are shown in Fig. 6. First, planar layers with a slight oversize in the x-direction are printed up to a predefined layer. For the tool change, a breakpoint was included in the g-code during the print preparation.

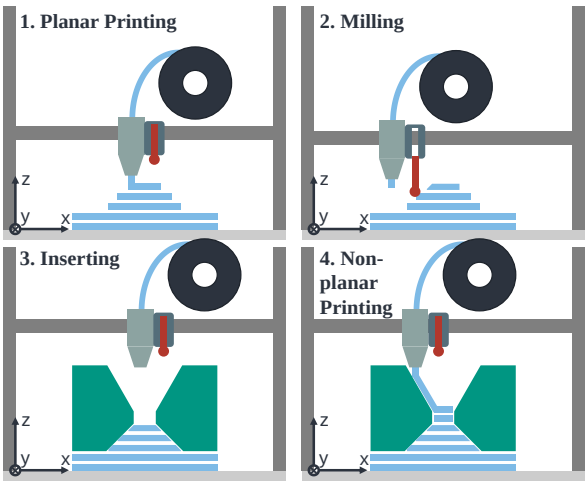

Figure 6. Additive-subtractive production of the sub-demonstrator.

Then a milling cutter is extended and the oversize is milled off, eliminating the stair-step effect. In the third step,

the inserts can be inserted with a precise fit without air pockets due to the stair-step effects. In the fourth step, the inserts are overprinted with non-planar layers, so that no stair-stepping effect occurs in the interface between FFF component and the insert.

IV. Results

A. Increased Manufacturing Accuracy

The following table shows the measurement results of the used coordinate measuring machine with the target value, actual value, deviation and the optimized results after one correction for the test workpiece. All data are in millimeters.

TABLE IV. Results of the Indirect Measurement Analysis

Feature	Target	Actual	Deviation	Optimized
P01	0.000	0.417	0.417	0.051
P02	0.000	0.863	0.863	0.207
P03	16.00	16.429	0.429	16.043
P04	16.00	16.3784	0.3784	16.027
P05	2.00	2.013	0.013	1.998

As seen in Table IV, the system's working accuracy was increased by correcting the distances (resolution 0.01 mm) between the nozzles and the milling tool in the CNC control. The remaining inaccuracies can probably be attributed to thermal effects (distortion on the component). During the entire process, the build platform is tempered to 75 ℃ to ensure secure adhesion during machining. After removing the part from the build platform, the component cools down uncontrollably, causing the component to warp. The following Fig. 7 also shows the visual effect of optimizing the working accuracy.

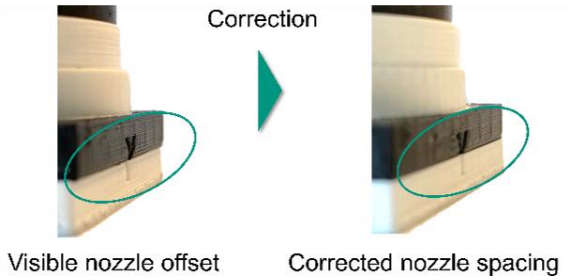

Figure 7. Influence of incorrect nozzle spacing for the test workpiece.

The influence of incorrect nozzle spacing can be seen in the illustration on the left. A step between the white PLA (nozzle 1) and the black PLA (nozzle 2) can be detected. In the illustration on the right, no step can be seen after correcting the nozzle distances.

During the experiments, it was found that the working accuracy could be successfully increased, but the production time was about 30% longer compared to commercially available FFF printers. The reasons for this are the more massive construction of the 4K FFF system and the associated higher mass inertia of the 4-axis gantry. This solid construction is advantageous for machining but disadvantageous for multi-material FFF printing.

B. Production of the Sub-demonstrator

Fig. 8 shows the sub-demonstrator with integrated SLA inserts (405 nm LCD UV Resin, ELEGOO) produced using three different printing strategies. In the case of complete planar layers for the FFF component, large gaps occur in the area of the lower interface between the SLA insert (light brown) and the FFF component (PLA material, white) due to the step effect. Gaps also occur in the upper interface area, therefore, insufficient adhesion can be assumed in this area. If, on the opposite, the upper interface layers are printed non-planar, the adhesion is significantly better, as the filaments are placed directly on the surface of the SLA insert during printing. As a result, the deposited filaments follow the contour of the insert. Although there is no step effect, even with non-planar printing gaps continue to appear in the lower interface. This can be attributed to the geometric imprecision and grooving of non-planar printing strategy, which makes a non-planar layer unsuitable for precise insert placement.

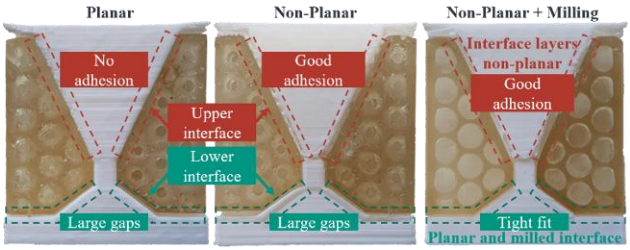

Figure 8. Comparison of fully planar and non-planar 3D-printing and milling.

If the sub-demonstrator is manufactured as described in Fig. 6, the best integration result is achieved. To ensure a tight fit of the SLA insert, the stair step effect in the lower interface is milled off. (see Fig. 8 on the right). In order to achieve good adhesion of the SLA insert and to avoid a step effect, the upper interface layers are still printed non-planar. A more detailed investigation of the adhesion performance of the material combination of PLA and SLA was carried out in a previous work [17]. The lessons learned from the fabrication of the sub-demonstrator were applied to the fabrication of the entire demonstrator. For this purpose, the lower chamfers of the ribs (lower interface to the pole shoes, see Fig. 5) are printed planar and milled to size before the pole shoes are integrated. In the next step, the middle parts of the rips are also built up planar until the height of the upper chamfers of the ribs (upper interface to the pole shoes) is reached. Finally, the pole shoes are overprinted non-planar to achieve a good adhesion in the interface. The result can be seen in Fig. 9.

A cut-out segment is used to show the successful and accurate integration of the heat sink and the pole shoes (see Fig. 9). Manufacturing attempts without milling of the lower interface resulted in the pole shoes standing too high and thus could not be overprinted. Manufacturing the demonstrator without a subtractive process step would therefore not be possible.

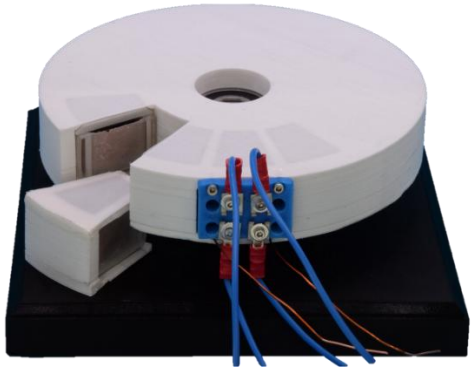

Figure 9. Demonstrator with segment cut out.

C. Discussion of the Results

The results in sections A and B clearly show that the interaction of the individual process steps is essential for the high-quality production of a hybrid polymer component. As expected, a central aspect is the dimensional accuracy of the FFF component. Here, a hybrid production system offers various possibilities to compensate for this shortcoming. On the one hand, a significant improvement of the basic FFF process can be achieved through an initial dimensional accuracy study with reference components. On the other hand, a further improvement is achieved by combining an optical analysis with a subtractive milling process. As the results show, this is particularly important for the contact surfaces of curved inserts. A non-planar printed support surface does not provide sufficient accuracy due to grooving during extrusion. However, the investigation of the non-planar layer deposition during overprinting shows a significantly better adhesion due to the reduced stair-step effect. It becomes clear that the greatest challenge in achieving the required dimensional accuracy lies in the interaction and correct use of the individual process steps. The analysis of the planar and non-planar layer deposition in particular was able to provide a clear statement in this regard.

V. Conclusion & Outlook

The stator of a double-sided axial flux machine was designed, considering the possibilities of functional integration when combining additive and subtractive processes. For a more straightforward illustration, a sub-demonstrator was derived, intended to show the advantages of targeted additive and subtractive manufacturing for the integration of inserts. A method was demonstrated to characterize and optimize the working accuracy between the additive and subtractive processes, and the results show increased accuracy. Using different techniques in the production of the sub-demonstrator showed where subtractive post-processing makes sense and where non-planar printing is advisable. The knowledge gained from manufacturing the sub-demonstrator was used to produce the demonstrator. Only the increased accuracy of the 4K FFF process and subtractive machining made it possible to manufacture the demonstrator with precise integration of various inserts.

Conflict of Interest

The authors declare no conflict of interest.

Author Contributions

Michael Baranowski, Sebastian Kleim and Nikolas Matkovic produced the demonstrator and the associated experiments; Marlies Springmann developed the flexible slicing strategy for generating the g-code; Adrian Schäfer and Marcel Waldhof carried out the construction and simulation of the stator. The results were reviewed and discussed by all authors. All authors wrote the paper and approved the final version.

Acknowledgment

The authors would like to thank the Ministry of Science, Research and Arts of the Federal State of Baden-Württemberg, Germany, for the financial support of the projects within the "InnovationsCampus Future Mobility" and for the possibility to conduct the investigations within the research campus.

References

[1] M. Waldhof, A. Echle, and N. Parspour, "A novel drive train concept for personalized upper body exoskeletons with a multiphase axial flux machine," in *Proc. 2019 IEEE International Electric Machines & Drives Conference (IEMDC)*, San Diego, CA, USA, 2019, pp. 2160–2166.

[2] B. Zhang, T. Epskamp, M. Doppelbauer, and M. Gregor, "A comparison of the transverse, axial and radial flux PM synchronous motors for electric vehicle," in *Proc. 2014 IEEE International Electric Vehicle Conference (IEVC)*, 2014, Florence, pp. 1–6.

[3] J. F. Gieras, R. J. Wang, and M. J. Kamper, *Axial Flux Permanent Magnet Brushless Machines*, New York, NY: Springer 2008.

[4] M. Springmann, N. Matkovic, A. Schäfer, M. Waldhof, T. Schlotthauer, M. Firedmann, M. Middendorf, J. Fleischer, and N. Parspour, "Flexible and high-precision integration of inserts by combining subtractive and non-planar additive manufacturing of polymers," *Key Engineering Materials*, vol. 926, pp. 268-279, 2022.

[5] Vansompel, H., Leijnen, and P. Sergeant, "Multiphysics analysis of a stator construction method in yokeless and segmented armature axial flux pm machines," *IEEE Transactions on Energy Conversion*, vol. 34, pp. 139–146, 2019.

[6] A. Di Gerlando, G. Foglia, M. Iacchetti, and R. F. Perini, "Parasitic currents in structural paths of yasa axial flux pm machines: estimation and tests," *IEEE Transactions on Energy Conversion*, vol. 31, pp. 750–758, 2016.

[7] B. Zhang, T. Seidler, R. Dierken, and M. Doppelbauer, "Development of a yokeless and segmented armature axial flux machine," *IEEE Transactions on Industrial Electronics*, pp. 1, 2015.

[8] J. Pyrhönen, T. Jokinen and V. Hrabovcová, *Design of Rotating Electrical Machines*, Chichester: Wiley 2008, pp. 540.

[9] B. Zhang, Y. Wang, M. Doppelbauer, and M. Gregor, "Mechanical construction and analysis of an axial flux segmented armature torus machine," in *Proc. 2014 XXI International Conference on Electrical Machines (ICEM)*, Berlin, Germany, 2014, pp. 1293–1299.

[10] A. Di Gerlando, G. M. Foglia, M. F. Iacchetti, and R. Perini, "Effects of manufacturing imperfections in concentrated coil axial flux PM machines: Evaluation and tests," *IEEE Transactions on Industrial Electronics*, vol. 61, pp. 5012–5024, 2014.

[11] M. Németh-Csóka, *Thermal Management of Electrical Machines, Measurement, Model and Energy Optimization, translated by Nikolas Matkovic*, Wiesbaden: Springer Fachmedien Wiesbaden 2018.

[12] R. Lehmann, M. Künzler, M. Moullion, and F. Gauterin, "Comparison of commonly used cooling concepts for electrical machines in automotive applications," *Machines*, p. 442, 2022.

[13] S. Oechslen, *Thermal Modelling of High Performance Electric Drives*, *Springer Vieweg*, Wiesbaden, Germany: 2018.
[14] P. Lindh, A. Jaatinen-Varri, A. Gronman, M. Martinez-Iturralde, *et al*., "Direct liquid cooling method verified with an axial-flux permanent-magnet traction machine prototype," *IEEE Transactions on Industrial Electronics 64*, pp. 6086–6095, 2017.
[15] R. Camilleri, and M.D. McCulloch, "Integrating a heat sink into concentrated wound coils to improve the current density of an axial flux, direct liquid cooled electrical machine with segmented stator," *Energies*, vol. 14, pp. 3619, 2021.
[16] J. Chang, Y. Fan, J. Wu, and B. Zhu, "A yokeless and segmented armature axial flux machine with novel cooling system for in-wheel traction applications," *IEEE Transactions on Industrial Electronics* 68, pp. 4131–4140, 2021.
[17] M. Baranowski, T. Schlotthauer, M. Netzer, P. Gönnheimer, and S. Coutandin, "Hybridization of fused filament fabrication components by stereolithographic manufactured thermoset inserts," *Recent Advances in Manufacturing Engineering and Processes. Proceedings of ICMEP*, Singapore: Springer Singapore Pte. Limited 2022, pp. 3–14, 2021.
[18] I. A. Tsekmes, R. Kochetov, P. Morshuis, and J. Smit, "Thermal conductivity of polymeric composites: A review," in *Proc. 2013 IEEE International Conference on Solid Dielectrics (ICSD)*, Bologna, Italy, pp. 678–681, 2013.
[19] M. Gräf, *Single-sided Transverse Flux Machine with Multifunctional Ceramic Support Ring*, Aachen: Shaker 2001.
[20] German Institute for Standardisation: DIN 8580:2022-12, Manufacturing processes-Terms and definitions, division. Berlin: Beuth Verlag GmbH, 2022.
[21] DMG MORI, LASERTEC 50 PrecisionTool. *LASERTEC Maschinen von DMG MORI*. [Online]. Available: https://de.dmgmori.com/produkte/maschinen/lasertec/lasertec-precisiontool/lasertec-50-precisiontool.
[22] Snapmaker EU, Snapmaker Artisan 3-in-1 3D-Drucker mit Gehäuse. [Online]. Available: https://eu.snapmaker.com/de/products/snapmaker-artisan-3-in-1-3d-printer?utm_campaign=artisan_product_release&gad=1&gclid=Cj0KCQjwr82iBhCuARIsAO0EAZzYf95QFI3Is0mexfs-kijpqiYFaP_EntmIkcfGYElxyDNeeXhG5nUaAgjDEALw_wcB
[23] Yamazaki Mazak UK Ltd., *Additive Manufacturing. Process Integration of Additive Manufacturing and Multi-Function Machining.* [Online]. [Available]: https://www.mazakeu.de/AM/
[24] S. J. Grunewald. (2016). Check Out this Awesome 5-Axis 3D Printer and Milling Machine Developed by Japanese Researchers. [Online]. Available: 3DPrint.com
[25] I. Gibson, D. Rosen, and B. Stucker, *Additive Manufacturing Technologies. 3d Printing, Rapid Prototyping and Direct Digital Manufacturing*, New York, Heidelberg, Dodrecht, London: Springer, 2015.
[26] A. Gebhardt, *Additive Fertigungsverfahren. Additive Manufacturing und 3D-Drucken für Prototyping, - Tooling – Produktion*, München, Hanser; Ciando, 2016.
[27] M. Baranowski, J. Schubert, K. T. Werkle, S. Schoner, and M. Friedmann, "Additive-subtractive manufacturing of multi-material sensor-integrated electric machines using the example of the transversal flux machine," in *Proc. IEEE 27th International Conference on Emerging Technologies and Factory Automation (ETFA)*, Stuttgart, Germany, pp. 1–4, 2022.
[28] F. Knoop, M. Köhler, V. Schöppner, and T. Lieneke, *Development of Design Rules for Hybrid Components: Integration of Metallic Inserts in FDM Structures, translated by Nikolas Matkovic*, *Konstruktion*, 2018.
[29] M. Baranowski, T. Schlotthauer, M. Netzer, P. Gönnheimer, S. Coutandin, *et al*., "Functional integration of subcomponents for hybridization of fused filament fabrication," 2022.
[30] M. Ankenbrand, Y. Eiche, and J. Franke, "Programming and evaluation of a multi-axis/multi-process manufacturing system for mechatronic integrated devices," in *Proc. International Conference on Electronics Packaging (ICEP)*, Japan, 2019.
[31] E. Aguilera, J. Ramos, D. Espalin, F. Cedillos, D. Muse, *et al*., "3D printing of electro mechanical systems," in *Proc. Solid Freeform Fabrication Symposium*, 2013.
[32] Y. Chang, K. Wang, C. Wu, Y. Chen, C. Zhang, *et al*., "A facile method for integrating direct-write devices into three-dimensional printed parts," *Smart Materials and Structures*, vol. 24, no. 6, pp. 65008, 2015.
[33] D. Espalin, D. W. Muse, E. MacDonald, and R. B. Wicker, "3D printing multifunctionality," *Structures with Electronics. The International Journal of Advanced Manufacturing Technology*, vol. 72, pp. 5–8, pp. 963–978, 2014.
[34] P. F. Flowers, C. Reyes, S. Ye, M. Kim, and B. J. Wiley, "3D printing electronic components and circuits with conductive thermoplastic filament," *Additive Manufacturing*, vol. 18, pp. 156–163, 2017.
[35] F. Wasserfall, "Embedding of SMD populated circuits into FDM printed objects," *Solid Freeform Fabrication Symposium*, pp. 1–10, 2015.
[36] F. Wasserfall, "Integration of conductive materials and SMD-components into the FDM printing process for direct embedding of electronic circuits," Ph.D. dissertation, University of Hamburg, 2019.
[37] S. Kleim, "Automation of an additive manufacturing machine for the production of functionally integrated polymer parts," Bachelor thesis, Karlsruhe Institute of Technology, 2020.
[38] M. Baranowski, N. Matkovic, F. Friedmann, and J. Fleischer, "3D-Druck für die Mobilität von morgen," *Werkstatttechnik 11/12*, pp. 807–811, 2021.
[39] I. Lorei, "Further development of a process planning tool to automate the control of hybrid additive-subtractive manufacturing process," Bachelor thesis, Karlsruhe Institute of Technology, 2022
[40] #3DBenchy, Measure and calibrate. [Online]. Available: https://www.3dbenchy.com/dimensions/
[41] A. Bandyopadhyay and B. Heer., "Additive manufacturing of multi-material structures," *Materials Science and Engineering: R: Reports*, vol. 129, pp. 1–16, 2018.
[42] S. N. Sanders, T. Schloemer, M. K. Gangishetty, D. Anderson, M. Seitz, *et al*., "Triplet fusion upconversion nanocapsules for volumetric 3D printing," *Nature 604* 7906, pp. 474–478, 2022.
[43] German Institute for Standardisation: DIN 66025-1:1983-01, Programme structure for numerically controlled working machines; general information. Berlin: Beuth Verlag GmbH
[44] International Organization for Standardization: ISO 6983-1:2009-12, Automation systems and integration - Numerical control of machines - Program format and definitions of address words - Part 1: Data format for positioning, line motion and contouring control systems. Berlin: Beuth Verlag GmbH
[45] M. Weck and C. Brecher, *Werkzeugmaschinen 5. Messtechnische Untersuchung und Beurteilung, Dynamische Stabilität*. Berlin, Heidelberg: Springer Berlin Heidelberg, 2006.